H. M. Karara
Y. I. Abdel-Aziz†
University of Illinois
Urbana, Illinois 61801

Accuracy Aspects of Non-Metric Imageries*

Opening the door to the use of non-metric cameras should enable many engineers and scientists to make full use of the technical and economical advantages of photogrammetry.

Abstract: *An updated version of the Direct Linear Transformation (DLT) emphasizes the mathematical modeling of lens distortions and film deformations. Experimental results indicate the levels of accuracy attainable at close range with four readily available non-metric cameras (Hasselblad 500 C, Honeywell Pentax Spotmatic, Crown Graphic, Kodak Instamatic 154) and the Hasselblad MK 70 metric camera. A technique compares the photogrammetric worthiness of measuring systems involving any camera (metric or non-metric). Expressions enable one to estimate the theoretically expected accuracies in object-space coordinates. The optimum number of object-space control points for the DLT solution is derived.*

Introduction

Research in close-range photogrammetry at the University of Illinois and elsewhere has clearly shown that[9,13], for numerous areas of applications and potential applications, fully acceptable accuracy can often be achieved with *better* non-metric cameras, such as Hasselblad, Robot, Linhof Technika, etc., provided that appropriate measures are taken in data acquisition and data reduction. Essentially, one has to: (a) choose a suitable configuration for data acquisition (b) provide the necessary object-space control, (c) counteract possible internal instability of the camera by combining calibration procedures with the measuring process, and (d) choose a suitable mathematical model to correct for the effect of lens distortions and film deformations. In view of the relatively large lens distortions and film deformations generally associated with non-metric cameras, the analytic approach has been almost exclusively used so far in photogrammetric data reduction from non-metric imageries.

In 1971 an analytic data reduction method, particularly suitable for non-metric imageries (*D*irect *L*inear *T*ransformation—DLT) was developed by the authors[1]. This method has since been used in numerous applications (e.g., by Williamson[14] and Faig[6,7] and others) and has proven its practical merits.

In this paper, an updated version of the DLT approach is discussed, with emphasis on the mathematical modeling of lens distortions and film deformations. A number of mathematical models have been investigated and the one deemed most suitable (on the basis of the experiments conducted and the statistical analysis undertaken) is recommended.

To the accuracy-conscious user of non-metric cameras, the experimental investigation (summarized later in the section, "The Photogrammetric Potential of Any Camera")

* Presented at the ASP/ACSM 1973 Fall National Convention, Orlando, Florida. Report on studies supported in part by the National Science Foundation (grant GK-11655).

† Currently a Research Associate, Biostereometrics Laboratory, Baylor College of Medicine, Houston, Texas 77025.

may be of some interest. These results indicate the levels of accuracy attainable with four readily available non-metric cameras (Hasselblad 500 C, Honeywell Pentax Spotmatic, Kodak Instamatic 154, Crown Graphic) as well as Hasselblad MK70.

Basic DLT Equations

As outlined in Reference 9, the basic equations for the Direct Linear Transformation method are:

$$x + \Delta x + \frac{l_1X + l_2Y + l_3Z + l_4}{l_9X + l_{10}Y + l_{11}Z + 1} = 0$$

$$y + \Delta y + \frac{l_5X + l_6Y + l_7Z + l_8}{l_9X + l_{10}Y + l_{11}Z + 1} = 0. \qquad (1)$$

where x,y are the comparator coordinates of an image point X,Y,Z are the object-space coordinates of that point, $l_1, l_2, \ldots, l_{11}$ are the transformation coefficients, and $\Delta x, \Delta y$ are image refinement components in x and y to account for the nonlinear components of lens distortions and film deformations.

In the linearized form, Equation 1 takes the following form:

$$A\, v_x + A\, \Delta x + x + l_1 X + l_2 Y + l_3 Z + l_4 + l_9\, x\, X + l_{10}\, x\, Y + l_{11}\, x\, Z = 0$$

$$A\, v_y + A\, \Delta_y + x + l_5 X + l_6 Y + l_7 Z + l_8 + l_o\, y\, X + l_{10}\, y\, Y + l_{11}\, y\, Z = 0 \qquad (2)$$

where $l_1, l_2, \ldots, l_{11}$ are transformation coefficients, $A = l_9 X + l_{10} Y + l_{11} Z + 1$, v_x, v_y are residual errors in image coordinates after refinement.

It should be pointed out that the linear components of lens distortion and film deformation are taken into account by the eleven transformation coefficients (l_1 through l_{11}) in Equation 2 in the process of transforming comparator coordinates into object-space coordinates. These linear components account for different scale factors along the x and y directions and for the nonperpendicularity of the comparator axes.

Image Refinement

The incorporation of provisions for image refinement (to account for the linear and the nonlinear components of lens distortions and film deformations) in data reduction is highly recommended if one wishes to obtain reasonably accurate results. In applications of low accuracy requirements, one may disregard Δx and Δy in Equation 2 where the nonlinear components of lens distortions and film deformation are not taken into account.

Lens Distortions

In an ideal lens with perfectly centered elements, lens distortion is strictly symmetrical about the optical axis. Errors in centering lens elements lead to asymmetrical lens distortion.

Symmetrical Lens Distortion. A generally accepted mathematical model for symmetrical lens distortion is an odd-powered polynomial:

$$\Delta r = k_1 r^3 + k_2 r^5 + \ldots + k_n r^{2n+1} \qquad (3)$$

where Δr is radial lens distortion, r is the length of the radial vector from the point of symmetry to the point under consideration, $r^2 = (x - x_s)^2 + (y - y_s)^2$, x,y are image coordinates of the point under consideration, x_s, y_s are image coordinates of the point of symmetry, and $(2n + 1)$ is the degree of the odd-powered polynomial.

Investigations have shown that, for the relatively simple lenses often used in non-metric cameras, k_1 is the only significant coefficient in Equation 3. Equation 3 can thus be reduced to:

$$\Delta r = kr^3. \qquad (4)$$

Asymmetrical Lens Distortion. A generally accepted mathematical model for asymmetrical lens distortion is the following one which reflects the distortion caused by decentering of lens elements and accounts for the selection of a point other than the point of symmetry as reference:

$$\Delta x = p_1 (r^2 + 2\bar{x}^2) + 2p_2\, \overline{xy}$$

$$\Delta y = p_2 (r^2 + 2\bar{y}^2) + 2p_1\, \overline{xy} \qquad (5)$$

where $\Delta x, \Delta y$ are asymmetrical lens distortion components, r is the length of the radial vector from the point of symmetry to the point under consideration, x,y are image coordinates of the point under consideration, referred to the point of symmetry, and p_1, p_2 are coefficients of asymmetrical lens distortion.

Film Deformations

Numerous sources contribute to film deformations in non-metric imageries including irregularities in film material, handling during processing, unflatness of the film inside the camera, tension exerted on the film inside the camera (between one photograph and another) and outside the camera (during processing), and temperature and relative humidity during storage of the film and during its processing.

Several mathematical models can be used to represent film deformations. To estimate the parameters of such models, one has to have some calibrated references (fiducial marks or reseau). In non-metric cameras, however, such references are generally not available and one can only use object-space control to determine the combined effect of film deformation and lens distortion. The estimates *RMS* values of the residual errors after image refinement, thus reflect, in this instance, unrepresented film deformations, unrepresented lens distortions and the random errors in measurement.

MATHEMATICAL MODELING OF IMAGE REFINEMENT

Models Tested. Based on the mathematical models used for film deformation and lens distortions in aerial cameras, and on results of experiments conducted by the authors[2], the following six mathematical models for image refinement in non-metric photography were selected for an experimental investigation.

Model I. Linear polynomial in x and y,

$$\Delta x = a_1 + a_2x + a_3y$$
$$\Delta y = a_4 + a_5x + a_6y. \qquad (6)$$

In this model, only the linear components of lens distortion and film deformation are taken into consideration. The nonlinear components of image refinement are neglected. Equation 6 accounts for the lack of perpendicularity of the x and y axes and allows for different scale factors along the x and y directions.

Incorporating Model I in Equation 2 does not change the form of the equations. In other words, the unknowns in the DLT solution using Model I remain as 11 unknowns. This should not be surprising as Equation 2, as stated earlier, takes into account the linear components of image refinement, in the process of transforming comparator coordinates into object-space coordinates. In combining the two sets of Equations 6 and 2, the six coefficients in Equation 6 thus absorbed by the 11 coefficients in Equation 2.

Model II. One more unknown (k_1) is added to Model I to account for symmetrical lens distortion,

$$\Delta x = a_1 + a_2x + a_3y + \bar{x}\, k_1r^2$$
$$\Delta y = a_4 + a_5x + a_6y + \bar{y}\, k_1r^2. \qquad (7)$$

in which the terms are defined after Equation 11. In this instance, the DLT solution involves 12 unknowns.

Model III. An odd radial polynomial of the seventh degree is added to Model I to account for symmetrical lens distortion,

$$\Delta x = a_1 + a_2x + a_3y + \bar{x}\,(k_1r^2 + k_2r^4 + k_3r^6)$$
$$\Delta y = a_4 + a_5x + a_6y + \bar{y}\,(k_1r^2 + k_2r^4 + k_3r^6). \qquad (8)$$

The DLT solution in this instance involves 14 unknowns.

Model IV. Model III is combined with Conrady's model[5] for asymmetrical lens distortion,

$$\Delta x = a_1 + a_2x + a_3y + \bar{x}\,(k_1r^2 + k_2r^4 + k_3r^6) + P_1(r^2 + 2\bar{x}^2) + 2P_2\,\overline{xy}$$
$$\Delta y = a_4 + a_5x + a_6y + \bar{y}\,(k_1r^2 + k_2r^4 + k_3r^6) + P_2(r^2 + 2\bar{y}^2) + 2P_1\overline{xy}. \qquad (9)$$

The DLT solution here involves 16 unknowns.

Model V. The same as Model IV, except the radial polynomial accounting for lens distortion is a full polynomial of the seventh degree,

$$\Delta x = a_1 + a_2x + a_3y + \bar{x}\,(k_1r^2 + k_2r^3 + k_3r^4 + k_4r^5 + k_5r^6) + P_1(r^2 + 2\bar{x}^2) + 2P_2\,\overline{xy}$$
$$\Delta y = a_4 + a_5x + a_6y + \bar{y}\,(k_1r^2 + k_2r^3 + k_3r^4 + k_4r^5 + k_5r^6) + P_2(r^2 + 2\bar{y}^2) + 2P_1\,\overline{xy}\ . \qquad (10)$$

Here the DLT solution involves 18 unknowns.

Model VI. Same as Model V, except the polynomial in x and y is of the second degree, accounting for the nonlinear component of film deformation,

$$\Delta x = a_1 + a_2x + a_3y + a_4x^2 + a_5y^2 + \bar{x}\,(k_1r^2 + k_2r^3 + k_3r^4 + k_4r^5 + k_5r^6) + P_1(r^2 + 2\bar{x}^2) + 2P_2\,\overline{xy}$$
$$\Delta y = a_6 + a_7x + a_8y + a_9x^2 + a_{10}y^2 + \bar{y}\,(k_1r^2 + k_2r^3 + k_3r^4 + k_4r^5 + k_5r^6) + P_2(r^2 + 2\bar{y}^2) + 2P_1\,\overline{xy}\ . \qquad (11)$$

In this model, the DLT solution involves 22 unknowns.

In all the above models, x,y are the image coordinates of the point under consideration, x_s,y_s are the image coordinates of the point of symmetry, $\bar{x} = x - x_s$, $\bar{y} = y - y_s$, r = length of the vector from the point of symmetry to the

TABLE 1. CAMERAS USED IN THE EXPERIMENTAL INVESTIGATION

Camera	Lens	Focal Length (mm)	Image Format (mm)	Approx. Price ($)
Kodak Instamatic 154	Kodak	43	12×12	15
Crown Graphic	Graphex f/4.7	135	120×100	300
Honeywell Pentax Spotmatic	Super Takumar f/1.4	50	36×24	500
Hasselblad 500 C	Planar f/2.8	80	55×55	550
Hasselblad MK 70	Biogon f/5.6 MK	60	55×55	4500

image point under consideration, $\Delta x, \Delta y$ = image refinement components, $a_1, a_2, \ldots a_{10}$ = coefficients of film deformation, $k_1, k_2, \ldots, k_5$ = coefficients of symmetrical lens distortion, p_1, p_2 = coeffcients of asymmetrical lens distortion.

Experimental Investigation. Five different cameras (Kodak Instamatic 154, Honeywell Pentax Spotmatic, Graflex, Hasselblad 500 C and Hasselblad MK 70) were used to investigate and compare the six above image refinement models. The image format, focal length of the lens used and the price (1973) are listed in Table 1 for each of the five cameras used. Kodak Plus X film was used in all the cameras except Hasselblad MK 70 where Kodak Tri X film was used.

Ten photographs were taken with each of the five cameras of a test area in which targets of known spatial position were placed mainly in two planes (Figure 1); a total of 39 targets were used (16 in Plane No. 1, 17 in Plane No. 2, and 6 scattered throughout the test area). For each camera, five of the photographs were taken from Camera Station No. 1 and five from Camera Station No. 2 (refer to Figure 1). The cameras were hand-held with their axes approximately horizontal and with convergence of about 30° ($\phi_1 \simeq \phi_2 \simeq 15°$ as sketched in Figure 1). In each instance, the stereobase was approximately 400 cm. The object distance for Plane No. 1 was approximately 550 cm and for Plane No. 2 approximately 400 cm, as sketched in Figure 1.

The *RMS* values of image plane residual errors (after image refinement) for each of the 50 resulting photographs are listed in Tables 2 through 7.

Discussion of Results. On the basis of the results tabulated in Tables 2 through 7, one can deduce as follows.

A. Regarding modeling of lens distortions.

(1) No significant improvement in accuracy is achieved by representing the lens distortion by a full polynomial rather than an odd polynomial (compare results of Model III with those of Model VI).

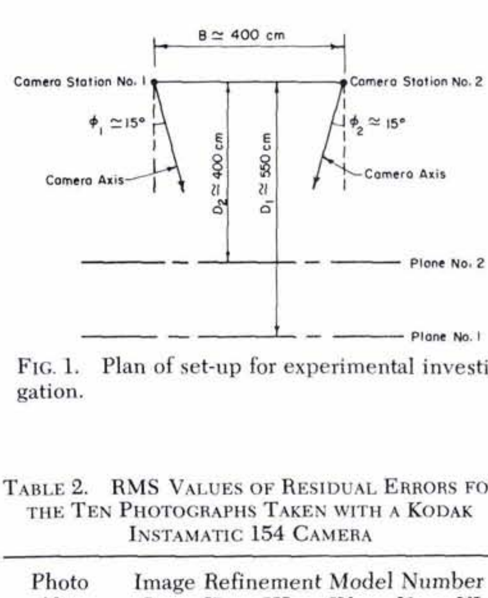

FIG. 1. Plan of set-up for experimental investigation.

TABLE 2. RMS VALUES OF RESIDUAL ERRORS FOR THE TEN PHOTOGRAPHS TAKEN WITH A KODAK INSTAMATIC 154 CAMERA

Photo No.	Image Refinement Model Number I (μm)	II (μm)	III (μm)	IV (μm)	V (μm)	VI (μm)
1	53.6	13.0	13.2	12.7	12.7	12.6
2	48.3	13.7	13.9	12.1	11.3	11.3
3	48.6	13.0	13.3	12.9	13.2	12.6
4	37.0	15.2	14.8	14.1	14.0	13.4
5	51.3	13.9	12.5	10.9	11.4	11.8
6	39.0	16.1	16.4	14.7	15.0	7.4
7	43.6	15.1	15.2	15.4	15.8	15.0
8	37.4	18.5	18.3	18.4	18.7	18.1
9	37.1	18.6	19.0	19.0	18.9	18.1
10	27.6	13.2	13.4	12.4	12.3	11.1
Mean RMS Value	43.0	15.2	15.2	14.5	14.6	13.5

TABLE 3. RMS VALUES OF RESIDUAL ERRORS FOR THE TEN PHOTOGRAPHS TAKEN WITH A CROWN GRAPHIC CAMERA

Photo No.	Image Refinement Model Number					
	I (μm)	II (μm)	III (μm)	IV (μm)	V (μm)	VI (μm)
1	12.9	5.8	4.8	4.8	4.7	4.0
2	16.9	9.3	8.4	8.4	8.2	7.1
3	17.2	14.5	11.9	11.8	11.7	11.8
4	23.6	12.2	10.2	10.3	10.3	8.2
5	24.4	12.6	12.2	12.2	12.0	8.6
6	23.8	15.2	13.5	13.6	12.3	9.2
7	17.2	10.7	8.8	8.6	8.8	7.2
8	14.7	11.6	7.6	7.6	7.7	7.6
9	18.2	11.7	8.8	8.8	8.8	7.6
10	9.2	8.6	6.6	6.6	6.6	5.8
Mean RMS Value	18.4	11.5	9.6	9.3	9.4	8.0

TABLE 4. RMS VALUES OF RESIDUAL ERRORS FOR THE TEN PHOTOGRAPHS TAKEN WITH A HONEYWELL PENTAX SPOTMATIC CAMERA

Photo No.	Image Refinement Model Number					
	I (μm)	II (μm)	III (μm)	IV (μm)	V (μm)	VI (μm)
1	28.2	3.9	3.9	2.2	2.3	2.2
2	28.3	3.9	3.7	2.3	2.3	2.4
3	28.3	3.1	3.1	2.0	1.9	1.8
4	28.2	3.2	3.2	3.0	2.7	2.5
5	26.1	3.8	3.7	3.8	3.9	3.7
6	29.5	4.0	4.0	4.0	4.0	3.9
7	30.3	4.7	4.8	4.3	4.2	4.3
8	24.6	3.8	4.0	2.8	2.8	2.8
9	23.1	4.2	4.3	3.5	3.6	3.2
10	22.4	4.4	4.5	3.3	3.4	3.2
Mean RMS Value	27.0	3.9	3.9	3.2	3.2	3.1

TABLE 5. RMS VALUES OF RESIDUAL ERRORS FOR THE TEN PHOTOGRAPHS TAKEN WITH A HASSELBLAD 500 C CAMERA

Photo No.	Image Refinement Model Number					
	I (μm)	II (μm)	III (μm)	IV (μm)	V (μm)	VI (μm)
1	28.8	3.6	2.4	3.4	3.5	3.0
2	30.3	4.9	4.8	4.6	4.5	4.0
3	28.4	6.2	5.5	5.4	5.4	5.2
4	29.4	3.6	3.4	3.5	3.5	3.3
5	25.2	7.6	7.6	7.3	6.7	6.4
6	34.2	6.7	6.7	6.8	5.9	6.0
7	34.5	7.1	7.0	6.8	6.4	6.0
8	28.4	6.6	6.8	6.9	7.0	6.4
9	28.6	5.0	4.9	4.8	4.8	4.7
10	28.8	7.8	7.9	8.0	8.2	7.7
Mean RMS Value	30.8	6.1	6.0	6.0	5.8	5.5

TABLE 6. RMS VALUES OF RESIDUAL ERRORS FOR THE TEN PHOTOGRAPHS TAKEN WITH HASSELBLAD MK 70 CAMERA. CALIBRATED RESEAU INTERSECTIONS WERE INCORPORATED IN THE IMAGE REFINEMENT.

Photo No.	Image Refinement Model Number					
	I (μm)	II (μm)	III (μm)	IV (μm)	V (μm)	VI (μm)
1	4.1	4.2	4.0	4.1	4.1	3.6
2	4.1	4.2	4.2	4.3	4.4	3.4
3	3.8	3.8	3.9	3.9	4.0	3.8
4	4.8	4.6	4.7	4.7	4.8	4.4
5	4.5	4.5	4.5	4.3	4.4	2.8
6	4.1	4.1	3.9	3.8	4.7	2.7
7	6.0	5.9	6.0	5.6	5.1	3.4
8	4.9	4.8	4.8	4.7	4.7	4.5
9	5.3	5.4	5.3	5.1	5.2	5.3
10	3.9	3.9	3.8	3.9	3.9	3.1
Mean RMS Value	4.6	4.6	4.6	4.5	4.5	3.8

(2) No significant improvement in accuracy is achieved by incorporating terms to account for asymmetrical lens distortion (compare Models III and IV).

(3) A statistical analysis of the results of the various models indicate that, for all the cameras tested except the Crown Graphic, only those unknowns involved in Model II are of significance in representing lens distortion. For the Crown Graphic camera, Model III showed a little improvement over Model II in that respect.

B. Regarding modeling of film deformations.

(1) No significant improvement in accuracy is gained by incorporating a second-degree polynomial to account for the non-linear components of film deformations (compare Models III and VI).

(2) For the Hasselblad MK 70, incorporating the calibrated coordinates of reseau intersections in the solution did not significantly improve the results (compare Tables 6 and 7).

C. Regarding the total DLT model.

On the basis of the above discussion, Model II is recommended for use in image refinement for non-metric photography. Model II (Equation 7) can be rewritten as:

TABLE 7. RMS VALUES OF RESIDUAL ERRORS FOR THE TEN PHOTOGRAPHS TAKEN WITH HASSELBLAD MK 70 CAMERA. CALIBRATED RESEAU INTERSECTIONS WERE NOT INCORPORATED IN IMAGE REFINEMENT.

Photo No.	Image Refinement Model Number I (μm)	II (μm)	III (μm)	IV (μm)	V (μm)	VI (μm)
1	4.7	4.1	4.1	4.2	4.2	3.4
2	4.8	4.3	4.4	4.5	4.6	3.6
3	4.9	4.7	4.5	4.2	4.4	3.8
4	6.3	5.0	5.1	5.1	5.2	4.6
5	5.7	5.7	5.7	5.8	5.8	3.9
6	3.7	3.8	3.8	3.7	3.8	3.1
7	5.9	5.9	6.0	6.1	5.5	4.5
8	5.9	5.9	5.7	5.8	5.7	5.3
9	5.8	5.8	5.4	5.5	5.5	5.0
10	4.7	4.6	4.6	4.6	4.5	4.2
Mean RMS Value	5.3	5.0	5.0	5.0	5.0	4.2

$$\Delta x = a_1 + a_2 x + a_3 y + \bar{x}\, k_1 \left\{(x-x_s)^2 + (y-y_s)^2\right\}$$

$$\Delta y = a_4 + a_5 x + a_6 y + \bar{y}\, k_1 \left\{(x-x_s)^2 + (y-y_s)^2\right\} \tag{12}$$

where x_s, y_s are image coordinates of the point of symmetry. (Approximate values for x_s and y_s can be determined from the approximate values of the DLT coefficients $(l_1, \ldots l_{11})$ using Equations 23 and 24 for x_o and y_o.)

With Model II chosen for image refinement, the DLT basic equation (Equation 2) can be rewritten as:

$$Avx + A(x-x_s)\,Kr^2 + x + l_1X + l_2Y + l_3Z + l_4 + l_9xX + l_{10}xY + l_{11}xZ = 0$$

$$Avy + A(y-y_s)\,Kr^2 + y + l_5X + l_6Y + l_7Z + l_8 + l_9yX + l_{10}yY + l_{11}yZ = 0. \tag{13}$$

Equations 13 involves 12 unknowns $(l_1, l_2, \ldots, l_{11}, K)$. A minimum of 6 object-space control points, well distributed throughout object-space and known in X,Y,Z would be necessary for a unique solution. Naturally, redundant object-space control would be highly desirable. One must avoid having all object-space control points in one plane. As much deviation from the planar arrangement as can be allowed by depth of field considerations is highly recommended.

Optimum Number of Object-Space Control Points. Although six object-space control points provide a unique solution, the incorporation of more control points improves the reliability of the solution.

The reliability of the solution is indicated by the standard deviation of the standard deviation of object-space coordinates. This can be expressed as:

$$S_S = \frac{S}{\sqrt{[2(n-u)]}} \tag{14}$$

where S_S is the standard deviation of the standard deviations of object-space coordinates $(X,Y,$ or $Z)$, S is the standard deviation of object-space coordinates $(X,Y,$ or $Z)$, n is the number of observation (twice the number of object-space control points), and u is the number of unknowns (12 for the mathematical model adopted).

Computing S_S for different numbers of object-space control points P, one gets the values shown in Table 8. Graphically, the relationship between S_S and P is plotted in Figure 2. A study of Figure 2 indicates that beyond some 20 to 25 object-space control points, the improvement of the reliability of the solution is relatively small and in all probability not worth the effort of providing further control points.

CONFIGURATION OF DATA ACQUISITION SET-UP

The configuration of data acquisition plays a major role in the accuracy of object-space coordinates obtained. An interesting study on this topic was conducted by the authors[2]. Because of the practical relevance of this matter, however, the conclusions of this study are briefly summarized here.

According to the authors[2], the expected standard deviations of object-space coordinates can be expressed in the symmetrical situation (refer to Figure 3) as:

TABLE 8. THE STANDARD DEVIATION OF THE STANDARD DEVIATION OF OBJECT-SPACE COORDINATES (S_S) VERSUS THE NUMBER OF OBJECT-SPACE CONTROL POINTS (P) USED IN THE SOLUTION.

P	6	7	10	15	20	30	40	50	100
S_S	∞	0.5S	0.25S	0.17S	0.13S	0.10S	0.08S	0.07S	0.05S

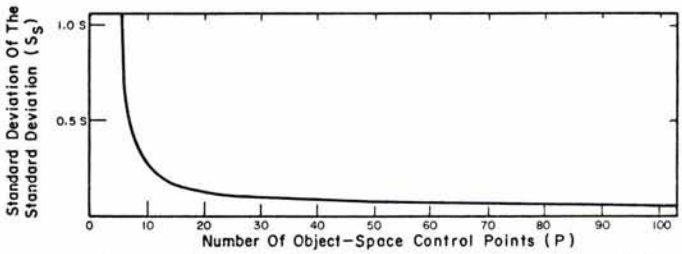

FIG. 2. The standard deviation of the standard deviation of the object-space coordinates S_S versus the number of object-space control points P used in the solution.

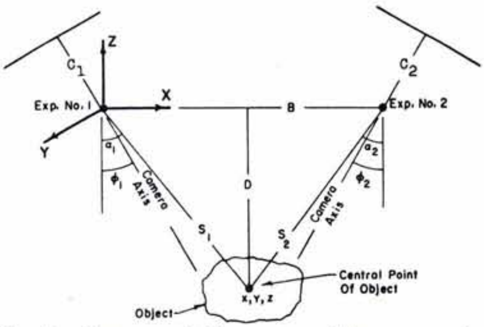

FIG. 3. Data acquisition set-up: The symmetrical case ($\phi_1 = \phi_2 = \phi$, $\alpha_1 = \alpha_2 = \alpha$ $C_1 = C_2 = C$).

$$m_Z = \frac{D/C}{B/D} \sqrt{2} \frac{(1 + \tan\alpha \tan\phi)}{(1 - \tan[\alpha-\phi] \tan\phi} m_x \quad (15)$$

$$m_x = \frac{D}{C} \frac{(1 + \tan\alpha \tan\phi)}{(1 - \tan[\alpha-\phi] \tan\phi} m_x \quad (16)$$

$$m_Y = \frac{D}{C} \frac{\sec \phi}{(1 - \tan[\alpha-\phi] \tan\phi)} m_x \quad (17)$$

$$m_T = \sqrt{(m^2{}_X + m^2{}_Y + m^2{}_Z)} \quad (18)$$

where m_X, m_Y, m_Z are the expected standard deviations in X,Y,Z object-space coordinates, m_T is the positional accuracy of object-space coordinates, $m_x = m_{x_1} = m_{x_2}$ is the accuracy of x image coordinate, $m_y = m_{y_1} = m_{y_2}$ is the accuracy of y image coordinate, x_1, y_1 are the image coordinates of image 1, x_2, y_2 are the image coordinates of image 2, $C = C_1 = C_2$ is the principal distance of the camera, D is the object distance to the central point of the object (as defined in Figure 3), B is the length of the base of the stereopair, $\phi = \phi_1 = \phi_2$ is half the value of the angle of convergence between the camera axes, and

$$\alpha = \alpha_1 = \alpha_2 = \tan^{-1}(B/2D) \quad (19)$$

From Equations 15 through 18, it is evident that m_X, m_Y, m_Z and m_T decrease (i.e., the accuracy of object-space coordinates improves) as the photo scale C/D increases.

From Equation 15, it is obvious that m_Z decreases as the ratio B/D increases. The maximum value of B/D can be obtained by maximizing B and minimizing D. The minimum value of D is limited by depth-of-field considerations, whereas the maximum value of B can be obtained in one of two ways:

- In the normal application of photogrammetry ($\phi=0$), one uses the minimum allowable overlap between the two photographs. For example, if A percent is the minimum overlap desired, and S the format size of the photographs, the maximum allowable value of base B would be:

$$B = \frac{D}{C} \; S \; \frac{(100-A)}{100} \quad (20)$$

- By using convergent photography. The accuracy of object-space coordinates, in this case, will also be a function of the value of the angle of convergence ϕ, as will be noted below.

Maintaining the B/D ratio fixed and changing ϕ, one finds that:

★ m_X, m_Y, m_Z, m_T increase as ϕ increases, as long as ϕ remains smaller than α (i.e., for $\phi < \alpha$),

★ m_X, m_Y, m_Z, m_T reach their maximum values if $\phi = \alpha$, and

★ m_X, m_Y, m_Z, m_T decrease as ϕ is increased beyond the value of α (i.e., for $\phi > \alpha$).

From the above discussion, it follows that the critical angle of convergence in the symmetrical case occurs at $\phi = \alpha$, i.e., if the camera axes are pointing to the central point in the object. By avoiding the critical angle of convergence (i.e., by choosing a value for the angle of convergence less or more than the critical value), one gets better results than those obtained where $\phi = \alpha$.

According to the authors[2], the most desirable configuration is the normal case. Should this not be feasible, convergent photography is to be utilized. The angle of convergence should be kept as small as possible and as far as possible from the critical value.

It should be pointed out that the authors[2] studied only the case of symmetrical convergence $(\phi_1 = \phi_2 = \phi)$. A study of the general case $(\phi_1 \neq \phi_2)$ is currently underway at the University of Illinois.

The Photogrammetric Potential of Any Camera

The photogrammetric potential of any camera is a function of the accuracy of the object-space coordinates obtained using the camera. As can be seen from Equations 15 through 18, the accuracy of object-space coordinates is a function of B, D, C, ϕ, m_x and m_y (α is not included because it is a function of B and D). These parameters can be divided into two groups:

- Parameters pertaining to the configuration of the data acquisition system: D, B, and ϕ.
- Parameters pertaining to the camera and to the data reduction system: C, m_x and m_y.

The effects of configuration parameters (D, B, ϕ) on the accuracy of object-space points were discussed in the previous section.

Theoretical and experimental studies were conducted to determine the standard deviations of object-space coordinates of targets photographed according to the configuration sketched in Figure 1 and discussed above. Tables 9 through 14 summarize the results of the experimental investigations. Referring to Figure 1, a total of 39 targets were measured (16 in Plane No. 1, 17 in Plane No. 2, and 6 placed throughout the test area).

Theoretical studies by the authors[2] showed that the accuracy of object-space coordinates is a function of the ratio m/C, where m is the average value of m_x and m_y, and C is the principal distance of the camera. The m/C ratio, referred to by the authors[2] as *angular error factor*, is suggested as a means to assign a numerical value to the photogrammetric worthiness of the total measuring system of which the camera is a part.

TABLE 9. ACCURACY (RMS) OF OBJECT-SPACE COORDINATES OBTAINED USING A KODAK INSTAMATIC 154 CAMERA

Stereo-model No.	Targets in Plane No. 1 (D = 550 cm)			Targets in Plane No. 2 (D = 400 cm)		
	σ_X (mm)	σ_Y (mm)	σ_Z (mm)	σ_X (mm)	σ_Y (mm)	σ_Z (mm)
1	1.6	1.1	2.0	0.5	0.8	1.0
2	1.2	1.4	2.3	0.5	1.1	2.0
3	1.0	1.3	2.5	0.8	0.8	1.6
4	1.6	1.5	3.5	0.7	0.9	2.0
5	1.0	1.3	2.4	0.6	0.7	0.8
Mean RMS Value	1.3	1.3	2.5	0.6	0.9	1.5

TABLE 10. ACCURACY (RMS) OF OBJECT-SPACE COORDINATES OBTAINED USING A CROWN GRAPHIC CAMERA

Stereo-model No.	Targets in Plane No. 1 (D = 550 cm)			Targets in Plane No. 2 (D = 400 cm)		
	σ_X (mm)	σ_Y (mm)	σ_Z (mm)	σ_X (mm)	σ_Y (mm)	σ_Z (mm)
1	0.28	0.27	0.93	0.22	0.09	0.36
2	0.55	0.53	1.43	0.26	0.19	0.58
3	0.41	0.26	1.00	0.12	0.07	0.31
4	0.37	0.28	1.71	0.15	0.12	0.67
5	0.43	0.38	1.38	0.16	0.20	0.38
Mean RMS Value	0.41	0.34	1.29	0.18	0.13	0.46

Obviously, the lower the value of m/C, the more appropriate is the measuring system for photogrammetric purposes.

The theoretical accuracy expected in object-space coordinates can be estimated by substituting the values of $B, D, \phi, \alpha, C, m_x$ and m_y in Equations 15 through 18. The values of m_x and m_y may be determined through comparator measurements or may be estimated on the basis of previous similar work. The value of C is obtained as a by-product of DLT solution as explained below.

For any object distance D, the value of the principal distance C is determined as a by-product of the DLT solution using the equations,

TABLE 11. ACCURACY (RMS) OF OBJECT-SPACE COORDINATES OBTAINED USING A HONEYWELL PENTAX SPOTMATIC CAMERA

Stereo-model No.	Targets in Plane No. 1 (D = 550 cm)			Targets in Plane No. 2 (D = 400 cm)		
	σ_X (mm)	σ_Y (mm)	σ_Z (mm)	σ_X (mm)	σ_Y (mm)	σ_Z (mm)
1	0.17	0.23	0.63	0.24	0.19	0.75
2	0.27	0.27	0.82	0.33	0.12	0.74
3	0.28	0.21	0.72	0.24	0.23	0.64
4	0.30	0.26	0.80	0.25	0.23	0.65
5	0.25	0.24	0.75	0.33	0.16	0.65
Mean RMS Value	0.25	0.24	0.74	0.28	0.19	0.69

TABLE 12. ACCURACY (RMS) OF OBJECT-SPACE COORDINATES OBTAINED USING A HASSELBLAD 500 C CAMERA

Stereo-model No.	Targets in Plane No. 1 (D = 550 cm)			Targets in Plane No. 2 (D = 400 cm)		
	σ_X (mm)	σ_Y (mm)	σ_Z (mm)	σ_X (mm)	σ_Y (mm)	σ_Z (mm)
1	0.36	0.19	1.03	0.22	0.32	0.34
2	0.44	0.39	1.36	0.39	0.20	1.00
3	0.34	0.15	1.22	0.09	0.16	0.62
4	0.39	0.30	1.31	0.25	0.25	1.14
5	0.32	0.26	0.85	0.38	0.43	0.70
Mean RMS Value	0.37	0.26	1.15	0.27	0.27	0.76

TABLE 13. ACCURACY (RMS) OF OBJECT-SPACE COORDINATES OBTAINED USING A HASSELBLAD MK 70 CAMERA. CALIBRATED RESEAU INTERSECTIONS ARE INCORPORATED IN THE SOLUTION

Stereo-model No.	Targets in Plane No. 1 (D = 550 cm)			Targets in Plane No. 2 (D = 400 cm)		
	σ_X (mm)	σ_Y (mm)	σ_Z (mm)	σ_X (mm)	σ_Y (mm)	σ_Z (mm)
1	0.28	0.38	1.10	0.18	0.33	0.80
2	0.40	0.26	0.85	0.18	0.20	0.71
3	0.36	0.24	1.25	0.16	0.23	0.60
4	0.47	0.41	1.03	0.10	0.25	0.78
5	0.28	0.29	1.13	0.17	0.23	0.83
Mean RMS Value	0.36	0.32	1.07	0.16	0.25	0.74

TABLE 14. ACCURACY (RMS) OF OBJECT-SPACE COORDINATES OBTAINED USING A HASSELBLAD MK 70 CAMERA. CALIBRATED RESEAU INTERSECTION COORDINATES ARE NOT INCORPORATED IN THE SOLUTION.

Stereo-model No.	Targets in Plane No. 1 (D = 550 cm)			Targets in Plane No. 2 (D = 400 cm)		
	σ_X (mm)	σ_Y (mm)	σ_Z (mm)	σ_X (mm)	σ_Y (mm)	σ_Z (mm)
1	0.50	0.31	1.48	0.17	0.24	0.70
2	0.55	0.35	1.07	0.18	0.32	0.88
3	0.41	0.35	1.03	0.17	0.36	0.71
4	0.45	0.24	0.83	0.27	0.28	0.75
5	0.34	0.28	1.27	0.22	0.19	0.51
Mean RMS Value	0.45	0.31	1.14	0.20	0.28	0.71

$$C^2_x = x_o{}^2 + \frac{(l^2_1 + l^2_2 + l^2_3)}{(l^2_9 + l^2_{10} + l^2_{11})} \quad (21)$$

$$C^2_y = y_o{}^2 + \frac{(l^2_5 + l^2_6 + l^2_7)}{(l^2_9 + l^2_{10} + l^2_{11})} \quad (22)$$

after estimating the parameters x_o and y_o from

$$x_o = \frac{l_1 l_9 + l_2 l_{10} + l_3 l_{11}}{l^2_9 + l^2_{10} + l^2_{11}} \quad (23)$$

$$y_o = \frac{l_5 l_9 + l_6 l_{10} + l_7 l_{11}}{l^2_9 + l^2_{10} + l^2_{11}} \quad (24)$$

From the values of C_x and C_y (the values of the principal distance as computed in the x and y directions), a representative value for the principal distance C can be determined as,

$$C = \tfrac{1}{2}(C_x + C_y) \quad . \quad (25)$$

Table 15 lists the estimated accuracy (*RMS*) for object-space coordinates in the above outlined experiment. As can be seen by comparing Table 15 to Tables 9 through 14, the theoretically expected values fairly well correspond to the experimentally obtained results. In these comparisons, one should bear in mind the variations experienced in the *RMS* values of the residual errors in the different photographs taken by the same camera, as can be seen from Tables 2 through 7.

CONCLUDING REMARKS

In numerous areas of applications (and potential applications) of close-range photo-

TABLE 15. THEORETICALLY EXPECTED ACCURACY (RMS) OF OBJECT-SPACE COORDINATES

Camera	D = 550 cm			D = 400 cm		
	σ_X (mm)	σ_Y (mm)	σ_Z (mm)	σ_X (mm)	σ_Y (mm)	χ_Z (mm)
Kodak Instamatic 154	2.00	2.00	4.10	1.40	1.40	2.00
Crown Graphic	0.47	0.47	1.08	0.33	0.33	0.54
Honeywell Pentax Spotmatic	0.43	0.43	0.85	0.31	0.31	0.44
Hasselblad 500 C	0.43	0.43	0.98	0.31	0.31	0.49
Hasselblad MK 70, Case A*	0.42	0.42	0.96	0.30	0.30	0.49
Hasselblad MK 70, Case B†	0.49	0.49	1.12	0.34	0.34	0.55

* Calibrated reseau intersections incorporated in the solution.

† Calibrated reseau intersections not incorporated in solution.

grammetry, the accuracy levels indicated in Tables 9 through 14 are completely acceptable. In such instances, then, an appropriate non-metric camera can be used for data acquisition. It is interesting to note that, except for the Kodak Instamatic 154 camera, the accuracies achieved using the four other cameras are essentially in the same ballpark.

Lest we be misunderstood, we stress the fact that although we firmly believe, on the basis of experimental investigations such as the ones presented in this paper, there is a definite place for non-metric cameras in close-range photogrammetry, we equally firmly believe that such cameras should be used only if the accuracy requirements permit. We do not foresee that non-metric cameras will completely replace metric cameras in close-range photogrammetry. Each of these two types of cameras have advantages and disadvantages and have an important role in photogrammetry.

It seems to both authors that the time has come for a thorough reexamination of the *metric or none* stand which many photogrammetrists have heretofore rather piously adhered to. Opening the door to the use of non-metric cameras in photogrammetric work should enable many engineers and scientists in numerous fields to make full use of the technical and economical advantages of photogrammetry.

References

1. Abdel-Aziz, Y. I. and Karara, H. M., "Direct Linear Transformation from Comparator Coordinates into Object-Space Coordinates," *Proceedings of the Symposium on Close-Range Photogrammetry*, Urbana, Illinois, Jan. 1971.
2. Abdel-Aziz, Y. I. and Karara, H. M., "Photogrammetric Potentials of Non-Metric Cameras," Civil Engineering Studies, Photogrammetry Series No. 36, University of Illinois at Urbana-Champaign, 1973.
3. Brown, D. C., "Close-Range Camera Calibration," *Photogrammetric Engineering*, 37:8, Aug. 1971.
4. Brown, D. C., "Calibration of Close-Range Cameras," Invited Paper, Commission V, XII International Congress of Photogrammetry, Ottawa, Canada, 1972.
5. Conrady, A., "Decentering Lens Systems," *Monthly Notices of the Royal Astronomical Society*, Vol. 79, 1919.
6. Faig, W., "Photogrammetric Measurements of Hydraulic Surfaces," *Proceedings of the 37th Annual Meeting of the American Society of Photogrammetry*, March 1971.
7. Faig, W., "Single Camera Approaches in Close-Range Photogrammetry," *Proceedings of the 38th Annual Meeting of the American Society of Photogrammetry*, March 1972.
8. Karara, H. M., "On the Precision of Stereometric Systems," Civil Engineering Studies, Photogrammetry Series No. 15, University of Illinois at Urbana-Champaign, 1968.
9. Karara, H. M., "Simple Cameras for Close-Range Applications," *Photogrammetric Engineering*, 28:5, May 1972.
10. Kenefick, J. F., "Ultra-Precise Analytics," *Photogrammetric Engineering*, 37:11, Nov. 1971.
11. Kenefick, J. F., Gyer, M. S., and Harp, B. F., "Analytical Self-Calibration," *Photogrammetric Engineering*, 38:11, Nov. 1972.
12. Schwidefsky, K. and Kellner, H., "Darstellung der Verzeichnungsfehler Photographischer Objektive Durch Potenzreihen," *Bildmessung and Luftbildwesen*, 37:2, March 1969.
13. Schwidefsky, K., "Precision Photogrammetry at Close-Ranges With Simple Cameras," *Photogrammetric Record*, Oct. 1970.
14. Williamson, J. R., "Analytical Reduction of Underwater Photography," M. S. thesis, University of Illinois at Urbana-Champaign, 1972.